applied sciences

MDPI

Article

The Principle and Downhole Testing of Water Injection Exploration in Depleted Reservoirs

Jinpeng Xu [1,*], Hui Zhao [1], Bing Dong [2], Yi Li [1] and Chuang Wang [1]

[1] School of Resources and Geosciences, China University of Mining and Technology, Xuzhou 221116, China; tb23010022a41@cumt.edu.cn
[2] Anhui Wanbei Coal Power Group Co., Ltd., Suzhou 234000, China
* Correspondence: xjp319@126.com

Abstract: Coal mine water hazards are one of the five major natural disasters in mines, and water in depleted areas is the most serious form of water hazard causing casualties. The exploration of depleted areas, especially old tunnels, presents significant challenges, and achieving the required borehole density for exploration in depleted areas is difficult in reality. The authors of this paper previously applied for a patent titled "Water Injection Exploration Method for Depleted Areas Based on Stress Seepage Principle". In order to theoretically analyze the feasibility of the patented results and validate them in practice, we first analyze the stress distribution and seepage phenomena around the goaf theoretically, construct boreholes underground in Renlou Coal Mine, conducting on-site water injection tests for different zones (depleted areas, old tunnels, and general boreholes), and perform transient electromagnetic observations during the water injection tests. A total of 355 sets of water injection flow rate and pressure data were obtained from different zones in three different boreholes; permeability coefficients were calculated based on the measured data, and relevant diagrams were drawn. Through the analysis of water injection test data and theoretical analysis, the following conclusions were drawn: there are disturbances and stress reduction zones around depleted areas (old tunnels), and when the equivalent normal stress induced by water injection pressure is greater than zero, the permeability of fractures will increase significantly. Whether it is a borehole aimed at depleted areas or old tunnels, it shows the characteristic that the closer the distance to the depleted areas (old tunnels) is, the smaller the water injection pressure, and the larger the permeability coefficient. When water is injected into the disturbance and stress reduction zones of the depleted areas (old tunnels), the water injection pressure can decrease from 9–10 MPa to 3–4 MPa, and the permeability coefficient may even increase in quantity value. The phenomena of pressure reduction and increased permeability during water injection are significantly observable, indicating that the water injection exploration method for depleted areas based on the stress seepage principle is feasible and has practical significance.

Keywords: old goaf water; exploration; water injection test; stress seepage coupling

Academic Editor: Tiago Filipe da Silva Miranda

Received: 27 September 2024
Revised: 20 December 2024
Accepted: 30 December 2024
Published: 7 January 2025

Citation: Xu, J.; Zhao, H.; Dong, B.; Li, Y.; Wang, C. The Principle and Downhole Testing of Water Injection Exploration in Depleted Reservoirs. *Appl. Sci.* **2025**, *15*, 504. https://doi.org/10.3390/app15020504

1. Introduction

Mine water hazards are one of the five major natural disasters in coal mines, and among these, water hazards from depleted areas pose the highest risk of causing casualties [1,2]. Depleted water, originating from either the mine itself or neighboring mines, accumulates in the goaf or old mine workings during the mining process. Depleted water hazards are characterized by sudden large water volumes and are highly prone to causing

casualties [3]. Statistics show that in recent years, the number of casualties caused by depleted water in mine water hazard accidents in China has been the highest.

The occurrence of depleted water differs from layered groundwater aquifers and fractured aquifers, with complex distribution, various types, and poor regularity [4]. Therefore, the exploration of depleted water presents significant challenges. In recent years, many geophysical methods have been applied to explore depleted areas, including surface electrical methods, surface transient electromagnetic methods [5,6], 3D seismic methods, and underground methods such as downhole electrical methods and downhole transient electromagnetic methods. However, the ambiguity of geophysical methods inevitably affects their accuracy, which has yet to be confirmed by authoritative data. The resolution of geophysical methods and their ability to accurately detect smaller goafs (such as old tunnels) still need further discussion. Zhou [7] mentioned that traditional geophysical exploration techniques have low resolution, making it difficult to effectively identify deep and small-scale ore body structures, and are poorly adapted under complex geological conditions. For instance, the major depleted water hazard accident at Wangjialing Coal Mine occurred because only geophysical exploration was conducted without drilling [8], which failed to detect the depleted water.

In Europe and Russia, hydraulic fracturing with high-pressure water injection is mostly used to weaken the rock mass to prevent rockbursts [9]. But in regions such as Shanxi and Inner Mongolia of China, water injection tests can be used to probe old empty areas. Considering the complexity of depleted water exploration, it is required to conduct "exploration for every excavation" during tunneling, and drilling exploration is mandatory. According to the "Coal Mine Water Prevention and Control Regulations," when conducting advanced exploration for unclearly located depleted water, the final borehole distance should not exceed "3 m apart on the horizontal plane" [10] to prevent accidental exposure to old tunnels and subsequent depleted water hazards. However, in practice, this regulation is difficult to comply with due to the extensive drilling requirements, which is one of the reasons for the occurrence of depleted water hazards [11].

To address this issue and achieve effective exploration of depleted areas (especially old tunnels) with minimal drilling (even just one borehole), the author and their team proposed a water injection exploration method for depleted areas based on the principle of stress–seepage coupling, and applied for relevant patents (patent number ZL2014 1 0454295X). This method involves injecting water and observing changes in water pressure and flow rate to explore potential depleted areas. This paper will elucidate the principles of this method and introduce the underground experimental conditions.

2. Theoretical Analysis of Water Injection Exploration Method for Depleted Areas Based on Stress–Seepage Coupling Principle

Fractures are widely distributed in various coal-bearing strata, and the surrounding coal and rock formations in depleted areas primarily consist of fissure media. The permeability of fractured rock masses is related to the spatial distribution of the rock fractures, including factors such as fracture density, orientation, and connectivity, but it primarily depends on the permeability of each individual fracture [12,13]. The permeability of fractures in their original state is determined by factors such as fracture width. For instance, the typical formula for permeability of smooth fractures [14] is as follows:

$$K_f = \frac{g b^2}{12 v_w} \tag{1}$$

In the formula, g represents a constant; b stands for fracture width; and v_w represents the dynamic viscosity coefficient of water, which is also a constant. Additionally, the

fracture width b is influenced by both groundwater pressure and in situ stress. Building upon previous research [15–17], the combined effect of groundwater pressure and lateral stress is referred to as the equivalent normal stress. The equivalent normal stress can be simply expressed as

$$\sigma_{ne} = P_c - P_f \tag{2}$$

P_c represents the vertical fracture pressure, and P_f stands for internal water pressure. It is only when the equivalent normal stress exceeds zero that the permeability of fractures significantly increases [18,19]. Furthermore, considering the three-dimensional stress effects, research by Zhao and Zheng [20] indicates that the expression for the effective normal stress (σ_n) on fractures is as follows:

$$\sigma_n = \sigma_2 + \mu(\sigma_1 + \sigma_3) - \beta P \tag{3}$$

In the equation, σ_2 represents the stress perpendicular to the crack, while σ_1 and σ_3 are the stresses parallel to the crack. The pore pressure within the crack is denoted as P. μ denotes Poisson's ratio, and the coefficient β represents the ratio of the connected area within the crack to the total area.

Based on the above equation, the formula for the permeability coefficient of fractures considering the influence of three-dimensional stress and pore pressure can be derived. Similar formulas and patterns can also be found in other studies [21].

$$K_f = \frac{gb^2}{12\nu_w} e^{\frac{3\sigma_n}{K_n}} = \frac{gb^2}{12\nu_w} e^{\frac{3\{\beta P - [\sigma_2 + \mu(\sigma_1 + \sigma_3)]\}}{K_n}} \tag{4}$$

From this equation, it can be observed that when σ_n = 0, the permeability coefficient remains in its original state, and when σ_n is less than 0, the permeability coefficient will significantly increase.

In coal and rock layers near the goaf, due to the adjacent side of the goaf being in an unloading state, the horizontal stress perpendicular to the goaf will sharply decrease or even become zero. On the other hand, according to the relevant literature [22], the distribution of coal pillars near the goaf includes fractured zones, plastic zones, elastic zones, and original rock stress zones, with vertical stress reduction observed in fractured and plastic zones. Moreover, with time passing, the stress near the goaf side will further decrease. The literature [23] also suggests that the goaf side is in a stress reduction zone. Therefore, both horizontal and vertical stresses in the coal and rock layers near the goaf are reduced. When injecting water near the goaf, under the same water pressure conditions, the effective stress σ_n will significantly increase, leading to a significant increase in the permeability coefficient.

Utilizing this principle, we can employ water injection methods to explore and conduct advanced exploration for depleted areas or similar structural bodies. The literature [24] also suggests that the extent of the voided area and damage characteristics can be determined by measuring water injection during drilling. During tunneling, boreholes are constructed and water injection tests are performed. When significant anomalies in water pressure, water volume, and permeability are observed during the water injection test, it indicates the presence of depleted areas within a certain range.

Furthermore, in the coal wall close to the goaf, there are also disturbances and damages caused by mining activities. In the disturbed zone, fractures develop, and during water injection, sudden changes in water pressure and water volume may occur.

3. Underground Testing of Water Injection Advanced Exploration Method for Depleted Areas Based on Stress–Seepage Coupling Principle

3.1. Experimental Plan

The underground experiment was conducted at Renlou Coal Mine, Anhui North Coal and Electricity Group, which belongs to the Huainan Coalfield. The coal-bearing strata are from the Lower Shihezi Formation of the Permian System, with the main coal seams being the 31st, 51st, 72nd, 73rd, and 82nd coal seams. The experiment site selected was the −720 North Main Road of Renlou Coal Mine. This roadway is located about 20 m above the 82nd and 73rd coal seams, with the 73rd coal seam being partially excavated for the 7324S working face gallery, while the 72nd coal seam has been mined, leaving behind the goaf of the 7224S working face. Additionally, there is a bottom extraction roadway for the 7324S working face on the floor of the 82nd coal seam (see Figures 1 and 2 for their cross-sectional relationships).

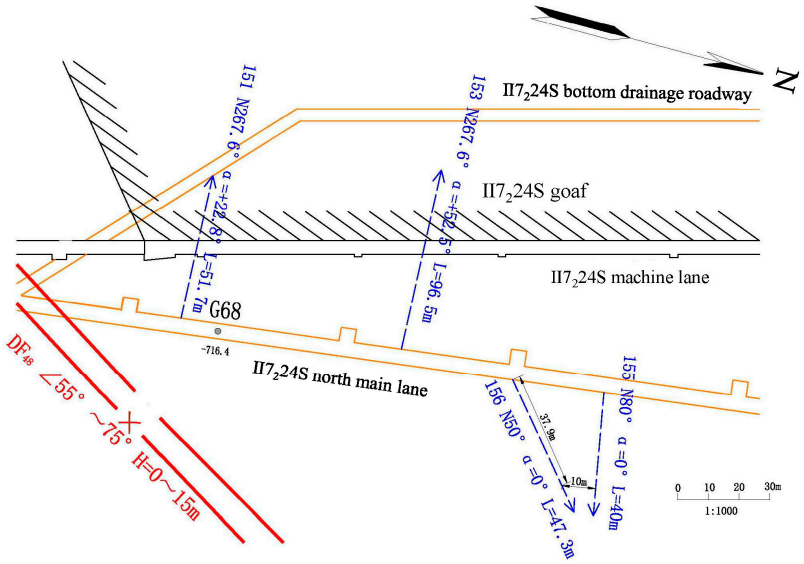

Figure 1. Water injection drilling plan.

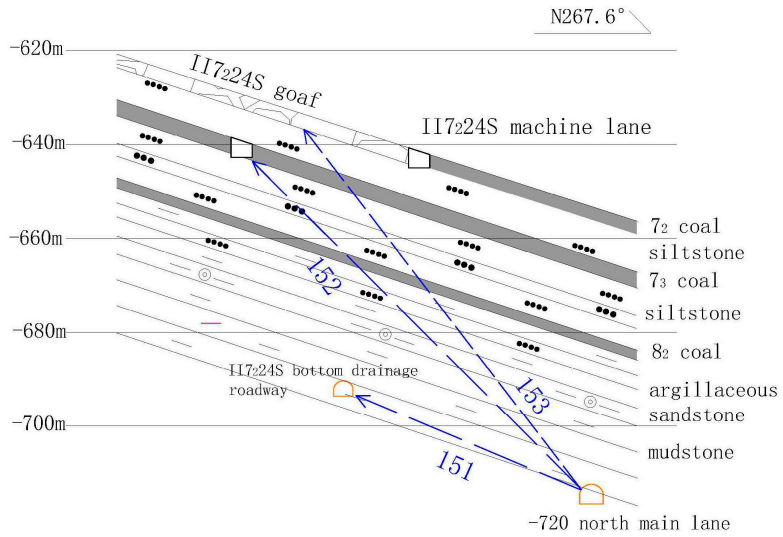

Figure 2. Borehole 151, 153 projection profile diagram.

The goaf of the 7224S working face and the bottom extraction roadway of the 7224S working face correspond to two different scenarios: goaf and old roadway. For these two situations, the 151st and 153rd holes are, respectively, designed for the goaf of the 7224S

working face and the bottom extraction roadway of the 7224S working face. Each hole has a diameter of 127 mm, with a casing set at 20 m depth, followed by grouting and solidifying of the casing, and then the diameter is reduced to 79 mm for further drilling. Water injection was carried out as required until the drilling target was reached. For further comparative analysis, holes 155 and 156 were designed, with hole 156 used for water injection and hole 155 for observation. Specific details of each borehole are shown in Figures 1–3, and other parameters such as hole positions are listed in Table 1.

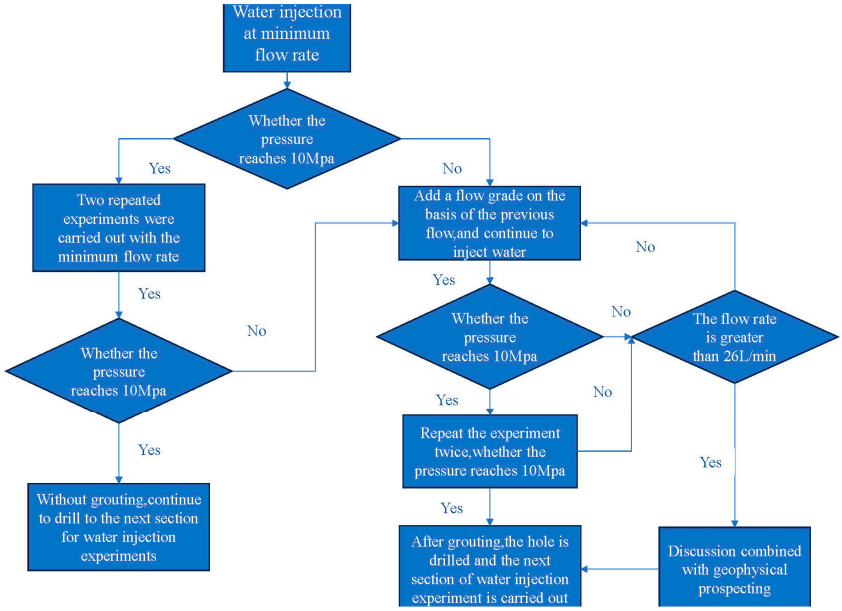

Figure 3. Water injection test flow chart.

Table 1. List of drilling parameters.

Hole Number	Opening Position	End Hole Target Point	Borehole Orientation ∠ (°)	Angle of Borehole ∠ (°)	Depth (m)
151	after G_{68} 12.5 m	Bottom pumping roadway of $7_3$24S	N267.6	22.8	51.7
153	before G_{68} 60 m	$7_2$24S working face goaf	N267.6	52.5	96.5
155	before G_{68} 127 m	156 holes	N80	0	40
156	before G_{68} 97 m	155 holes	N50	0	47.3

After the completion of each borehole, strict trajectory measurements were conducted, and the data indicated that the boreholes met the design requirements. During the drilling and water injection process, transient electromagnetic monitoring was simultaneously carried out.

3.2. Water Injection Test Process and Water Injection Data

This time, the water injection test used the method of simultaneous injection and reinforcement while drilling. A pneumatic grouting pump ZBQ16/12 was used in this experiment, with a maximum pressure of 12 MPa and a maximum flow rate of 26 L/min, and a minimum flow rate of 2 L/min. In the actual water injection process, water injection was first performed at the minimum flow rate while observing the pressure. If the pressure rose above 10 MPa (indicating that the seepage rate was less than 2 L/min, suggesting that this section had good resistance to water pressure), the check valve was closed, and pressure changes were observed. To ensure the reliability of the test data, two identical tests were conducted at the minimum flow rate again. If the results were the same, it indicated that this section indeed had resistance to water pressure, and the water injection

for this section could be terminated. Without grouting, drilling continued for another 4 m to enter the next section of water injection. If the pressure could not rise to 10 MPa during water injection at the minimum flow rate, observation was continued for 30 min. If after 30 min the pressure still could not reach 10 MPa, the flow rate was increased by one level. If the pressure rose above 10 MPa, two identical tests were conducted again as described above. If both tests reached the pressure, water injection for the next stage would begin, and post-grouting hole drilling was required. If the pressure could not rise to 10 MPa, observation continued for 30 min, and the flow rate was increased again, repeating the aforementioned test process. The water injection process is shown in Figure 3.

(1) Hole No. 151

The borehole underwent 4 stages of water injection tests. Injection was conducted at a depth of 31.7 m (with the test section being 20~24 m away from the roadway) using a flow rate of approximately 10 L/min. The water pressure reached around 10 MPa and remained stable, with a rock permeability coefficient of approximately 0.00275 m/d.

Continuing forward, injection was carried out at a depth of 35.7 m (with the test section being 16~20 m away from the roadway). Starting with a flow rate of 10.26 L/min, the flow rate was gradually increased. When the flow rate reached 23.76 L/min, the water pressure stabilized at around 6 MPa, and the permeability coefficient reached approximately 0.01080 m/d.

Proceeding further, injection was performed at a depth of 39.7 m (with the test section being 12~16 m away from the roadway). Injection started with a flow rate of 9.34 L/min and was gradually increased. When the maximum flow rate reached 27.31 L/min, the water pressure stabilized at around 5.6 MPa. At maximum flow, the permeability coefficient reached approximately 0.013202 m/d.

Continuing to drill to a depth of 43.7 m (with the test section being 8~12 m before reaching the end of the borehole), injection was carried out. At a flow rate of 11.53 L/min, the water pressure stabilized at around 5.07 MPa, and at a flow rate of 20.51 L/min, the water pressure stabilized at around 4.83 MPa. The permeability coefficient reached approximately 0.01080 m/d. Hole No. 151 underwent a total of 136 water injections, as detailed in Table 2.

Table 2. Hole 151 data statistics.

Distance Between Water Injection Section and Roadway (m)	Number of Water Injections		Flow Rate V (L/min)	Water Pressure P (MPa)	Permeability Coefficient P (MPa)
20~40	15	Min	8.31	9.4	0.00236
		Max	10.69	10	000297
		Average	9.81	9.72	0.00269
16~20	60	Min	9.02	4.8	0.00488
		Max	25.17	6.2	0.01109
		Average	17.01	5.78	0.00779
12~16	45	Min	8.31	4.39	0.00488
		Max	27.31	5.6	0.01302
		Average	11.55	5.02	0.00607
8~12	16	Min	8.31	4	0.00517
		Max	21.37	5.9	0.01189
		Average	16.32	4.95	0.00868

(2) Hole No. 153

Hole No. 153 underwent water injection in 5 sections at distances of 38~18 m from the old goaf (i.e., sections at distances of 38~34 m, 34~30 m, 30~26 m, 26~22 m, and 22~18 m from the old goaf). Due to the higher permeability in the 34~30 m section, to prevent it from affecting the effectiveness of the next injection section, grout sealing was conducted

in this section before proceeding with hole cleaning and continuing drilling into the next section for water injection testing. The specific water injection process was similar to that of Hole No. 151 and is not reiterated here. A total of 134 water injections were conducted in 5 sections, as detailed in Table 3.

Table 3. Hole 153 data statistics.

Distance Between Water Injection Section and Roadway (m)	Number of Water Injections		Flow Rate V (L/min)	Water Pressure P (MPa)	Permeability Coefficient P (MPa)
34~38	14	Min	8.07	9.45	0.00146
		Max	11.16	10.01	0.00191
		Average	9.88	9.73	0.00173
30~34	32	Min	9.02	4.95	0.00284
		Max	26.6	5.85	0.00881
		Average	15.93	5.33	0.00518
26~30	15	Min	2.37	8	0.00055
		Max	2.85	9.73	0.00093
		Average	2.58	8.89	0.00065
22~26	41	Min	13.54	8.4	0.00275
		Max	22.32	9.8	0.00424
		Average	18.62	9.3	0.00343

(3) Hole No. 156

This hole underwent water injection testing in three sections: 37.9~41.9 m, 41.9~45.9 m, and 45.9~47.3 m, with Hole No. 155 serving as the observation hole. During the three water injection tests, the flow rate increased according to the predetermined plan. A total of 85 water injections were conducted in three sections, with water injection pressure ranging from 4 to 6 MPa. Statistical data are detailed in Table 4.

Table 4. Hole 156 data statistics.

Distance Between Water Injection Section and Roadway (m)	Number of Water Injections		Flow Rate V (L/min)	Water Pressure P (MPa)	Permeability Coefficient P (MPa)
7.8~9.9	28	Min	9.97	4.98	0.00549
		Max	20.9	6.64	0.00872
		Average	16.13	5.68	0.00747
5.7~7.8	28	Min	12.35	4.99	0.00651
		Max	21.37	6.24	0.00912
		Average	16.705	5.6	0.00787
5~5.7	29	Min	11.4	4.58	0.00662
		Max	22.08	5.8	0.01016
		Average	16.32	5.215	0.00822

3.3. Geophysical Situation During Water Injection

During the water injection testing process, geophysical monitoring work was conducted simultaneously, specifically transient electromagnetic detection. The transient electromagnetic results from the left side of borehole 151 were selected for illustration (see Figure 4). During the water injection testing of the borehole, transient electromagnetic surveys were conducted along the azimuth and inclination directions of the borehole to characterize the electromagnetic field responses of the surrounding rock layers. By comparing and analyzing the contour profiles of the resistivity values of the intact rock layers before water injection and the contour profiles of the resistivity values after water injection at pressures of 4.5 MPa and 5.5 MPa, it was evident that the resistivity of the rock layers surrounding the borehole changed significantly after water injection.

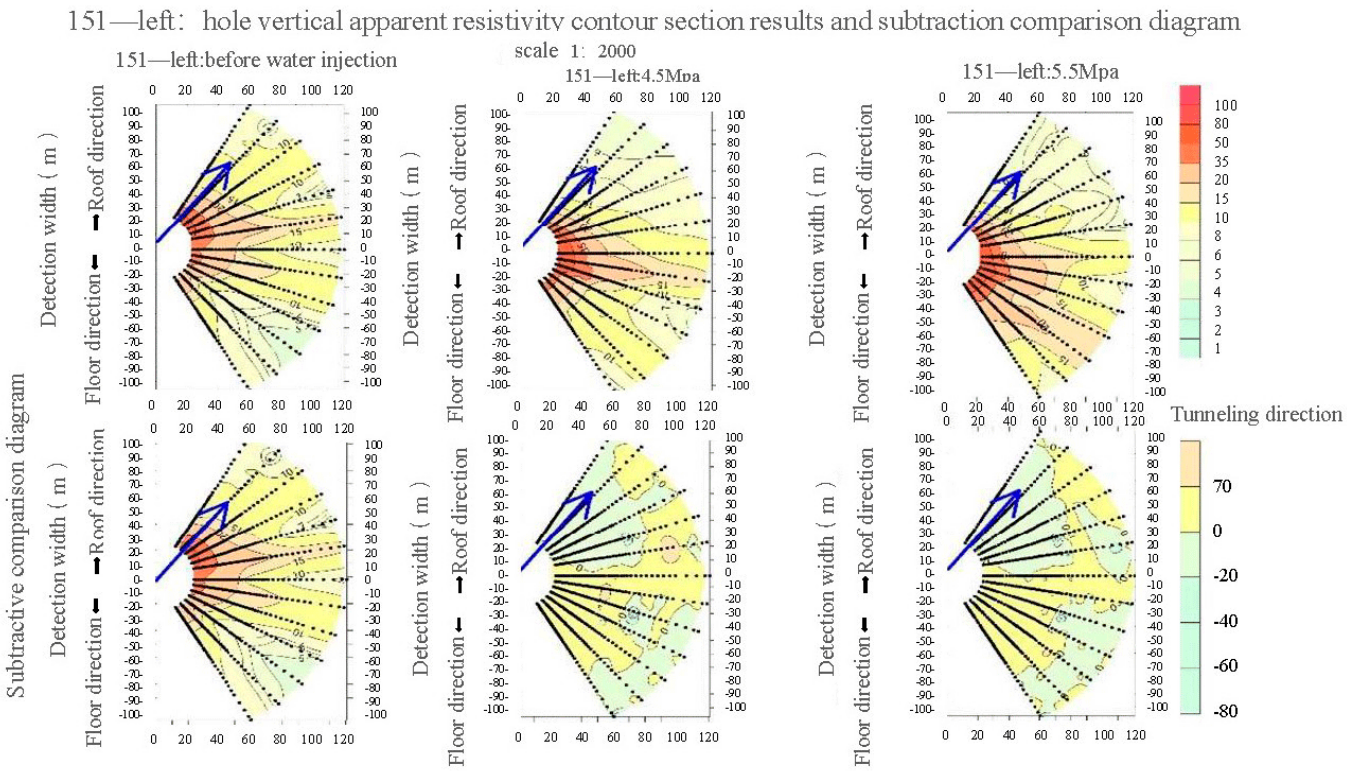

Figure 4. Comparison chart for 151—left: vertical apparent resistivity contour section results.

From Figure 4, the arrow indicates the direction of drilling, it can be observed that when the pressure reached 4.5 MPa, the top plate region of borehole 151 (left side) within the range of 10~90 m and the area in front of the borehole within the range of 20~80 m became low-resistivity zones. When the pressure reached 5.5 MPa, the top plate region of borehole 151 (left side) within the range of 0~90 m, the area in front of the borehole within the range of 20~80 m, and the range of 100~110 m turned into low-resistivity zones. Based on this, it can be inferred that high-pressure water has undergone a certain distance of seepage, leading to a decrease in resistivity in the original high-resistivity zone.

3.4. Analysis and Discussion of Water Injection Results

3.4.1. The Pressure–Permeability Patterns at Different Distances from the Old Goaf

Through the water injection tests conducted at boreholes 1# and 3#, it was observed that the maximum water pressure and permeability patterns varied at different distances from the old goaf. Curves depicting the flow rate and pressure at different injection points for the three boreholes were plotted separately (refer to Figures 5–7).

From Figure 5, it can be seen that at distances ranging from 24 m to 20 m from the old roadway, the water injection pressure ranged between 9 and 10 MPa; at distances ranging from 20 m to 16 m from the old roadway, the water injection pressure ranged between 5.8 and 6.4 MPa; at distances ranging from 16 m to 12 m from the old roadway, the water injection pressure ranged between 5.0 and 6.0 MPa; and at distances ranging from 12 m to 8 m from the old roadway, the water injection pressure decreased to 4 MPa. It is evident that the water injection pressure at borehole 151 decreased significantly as the distance from the old roadway decreased.

Figure 6 illustrates that at distances ranging from 38 m to 34 m from the old goaf, the water injection pressure ranged between 9 and 10 MPa; at distances ranging from 34 m to 30 m from the old goaf, the water injection pressure ranged between 5.4 and 6.0 MPa; at distances ranging from 30 m to 26 m and from 26 m to 22 m from the old goaf, the water injection pressure increased to between 8.0 and 9.0 MPa; and at distances ranging from

22 m to 18 m from the old goaf, the water injection pressure decreased to below 3 MPa. Analysis suggests that in the 30 m to 22 m segment, the abnormal water injection pressure was mainly due to grouting after the injection at 34 m to 30 m, resulting in the diffusion of grout into the 30 m to 22 m segment. However, overall, borehole 153 also exhibited the characteristic of decreasing water injection pressure with proximity to the old goaf.

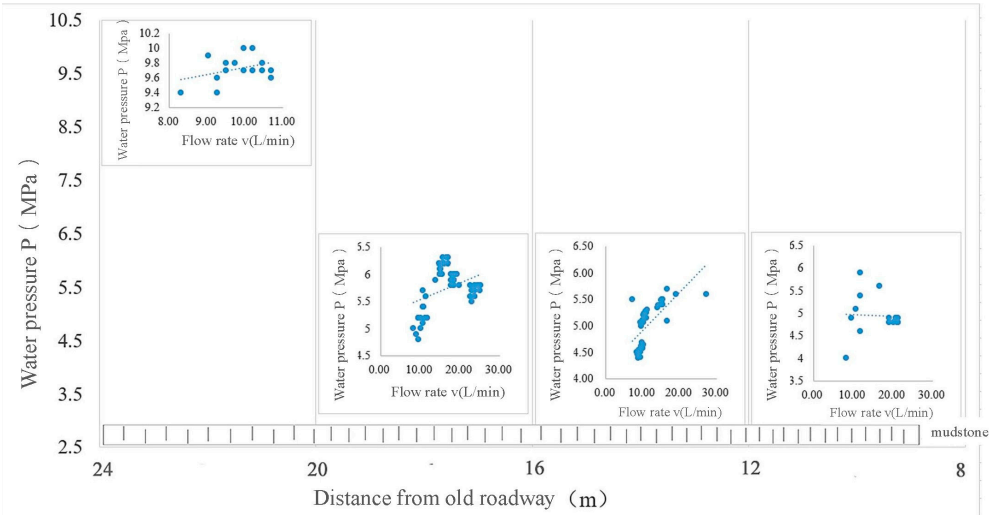

Figure 5. Water injection pressure and flow chart of different positions of hole 151.

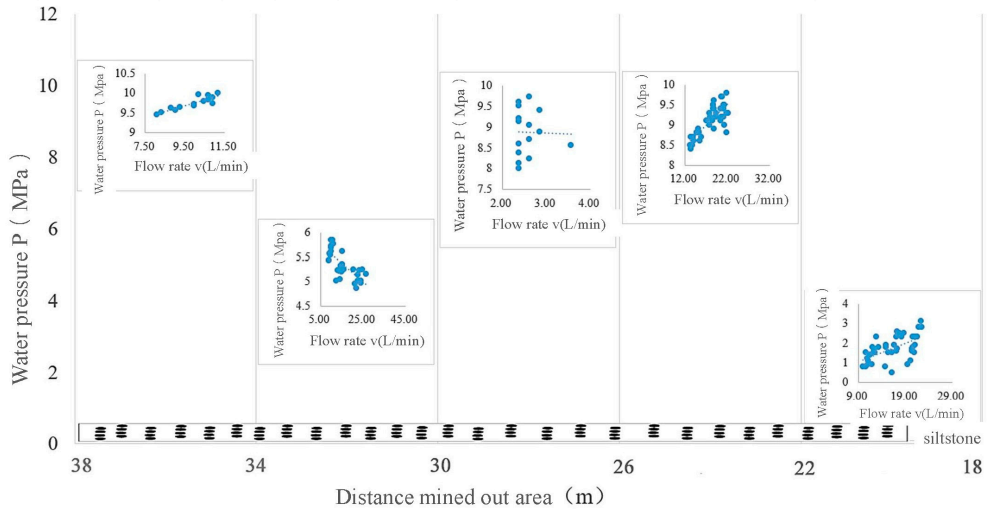

Figure 6. Water injection pressure and flow chart of different positions of hole 153.

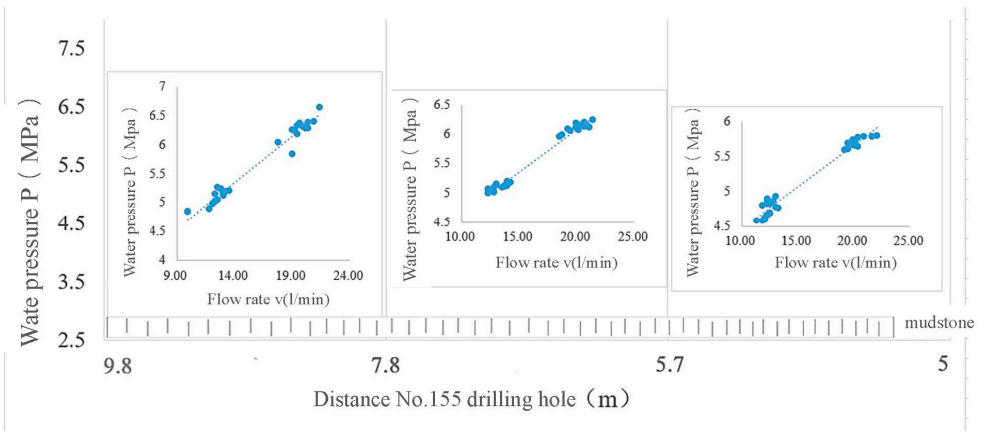

Figure 7. Water injection pressure and flow chart of different positions of hole 155.

From Figure 7, it can be observed that borehole 156, unaffected by the old goaf or old roadway, maintained relatively stable water injection pressure, ranging between 4.5 and 5 MPa.

3.4.2. The Permeability Patterns at Different Distances from the Old Goaf

When the injection point is at different distances from the old goaf, not only does the maximum injection pressure vary, but the permeability coefficient also shows differences. According to the injection test data, the permeability coefficient of the rock mass can be calculated using Formula (5) provided in the "Technical Code for Drilling Water Pressure Test of Water Conservancy and Hydropower Engineering" (NB/T35113-2018) issued by the Ministry of Water Resources [25].

$$K = \frac{Q}{2\pi HL} \ln \frac{L}{r_0} \tag{5}$$

In the formula, K represents the permeability coefficient of the rock mass, expressed in m/d; Q denotes the injection flow rate, measured in m^3/d; H stands for the head of the test water (which can be converted from water pressure), expressed in meters; L represents the length of the test section, measured in meters; and r_0 denotes the radius of the borehole, measured in meters.

Based on the calculated permeability coefficients, the flow rate and pressure curves for injections at different locations of the three boreholes were plotted separately (refer to Figures 8–10).

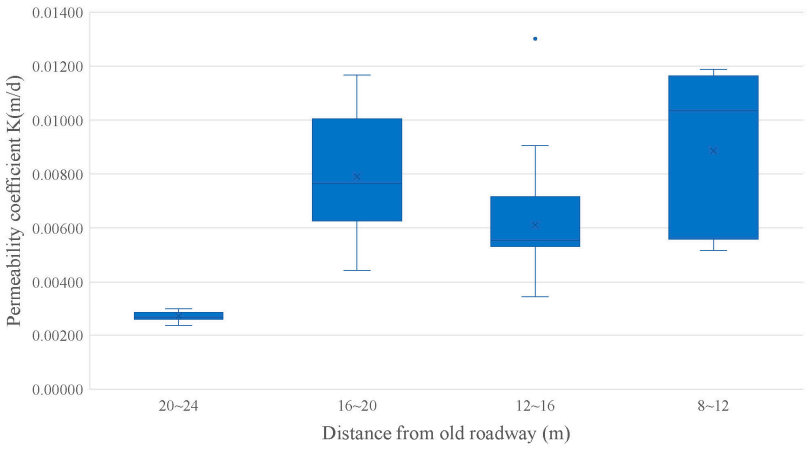

Figure 8. Box plot of permeability coefficient at different positions of borehole 151.

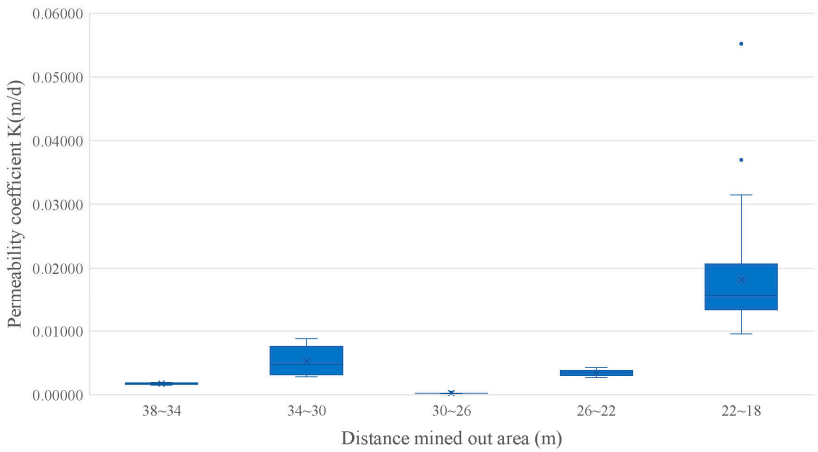

Figure 9. Box plot of permeability coefficient at different positions of borehole 153.

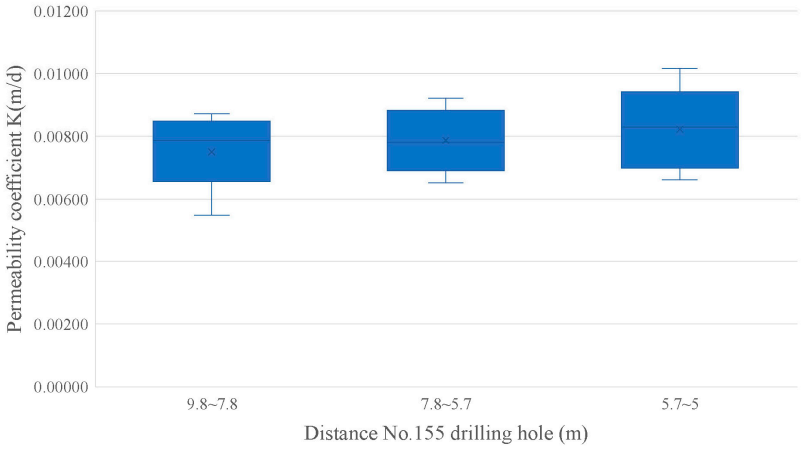

Figure 10. Box plot of permeability coefficient at different positions of borehole 155.

From Figure 8, it can be observed that the permeability coefficient exhibits a 2–3 times increase as the distance changes from the section 24–20 m from the old goaf to the section 20–16 m from the old goaf, and further to the section 16–12 m from the old goaf. The permeability coefficient overall tends to be greater in the section 12–8 m from the old goaf compared to the section 16–12 m from the old goaf. The permeability coefficient of borehole 151 demonstrates that the closer it is to the old goaf, the higher the permeability coefficient.

From Figure 9, it can be observed that the permeability coefficient significantly increases from the section 38–34 m from the old goaf to the section 34–30 m from the old goaf. However, in the sections 30–26 m and 26–22 m from the old goaf, the permeability coefficient decreases before rising again. In the section 22–18 m from the old goaf, the permeability coefficient experiences a significant increase by orders of magnitude, reaching below 0.01 m/d. It is seen that, similar to the abnormal water pressure, in the section 30–22 m from the old goaf, the injection of grouting after the injection from 34 to 30 m caused the grout to spread to the section 30–22 m from the old goaf, resulting in an abnormal permeability coefficient for injection, but, overall, borehole 153 also exhibits the characteristic that the closer it is to the old goaf, the higher the permeability coefficient.

From Figure 10, it can be seen that the permeability coefficient of borehole 156 does not undergo significant numerical changes, but overall, it also demonstrates the characteristic that the closer it is to borehole 155, the higher the permeability coefficient.

3.4.3. General Pattern Analysis

Based on the analysis above, whether near the goaf or near the old roadway, there is a phenomenon of decreasing water injection pressure and increasing permeability as the distance from the goaf decreases. The main reason for this phenomenon is the existence of pressure relief and disturbance damage near the goaf or old roadway.

In the original undamaged rock segment, the ground stress is normal (minimum stress greater than 10 MPa). The characteristics of water injection in this segment are as follows: the water injection pressure can be increased to 10 MPa, but the flow rate is very small and difficult to increase. The permeability is relatively small, as expected for the permeability of the original rock.

In the segment affected by pressure relief and disturbance near the goaf and old roadway, the surrounding rock stress decreases due to the pressure relief caused by the roadway or goaf (minimum stress less than 10 MPa, generally around 5 MPa). The characteristics of water injection in this segment are as follows: compared to the first segment, the pressure significantly attenuates, and the water injection pressure has difficult exceeding the surrounding rock pressure (5~6 MPa); the overall permeability is greater than the permeability

in the original state, and as the injection pressure increases, the natural fractures expand under the action of water injection, leading to a significant increase in permeability, even by an order of magnitude. Moreover, as the distance to the goaf (or old roadway) decreases, the water injection pressure decreases and the permeability increases.

Hole 151 indicates that within 20 m of the old roadway is an area affected by pressure relief and disturbance. Hole 153 indicates that within 34 m of the goaf is an area affected by pressure relief and disturbance. Hole 156 is within the pressure relief and disturbance zone during the injection stage (10 m from hole 155).

3.4.4. The Application Significance

Through the water injection experiments, further confirmation has been provided regarding the phenomena of disturbance damage and stress reduction near the depleted zones (old tunnels). These phenomena leads to the observed decrease in water pressure and increase in permeability during the water injection process. Conversely, these phenomena can also be utilized to investigate disturbance damage and stress reduction, thereby facilitating the exploration of depleted zones and old water zones. The water injection experiments also demonstrate that the decrease in pressure and increase in permeability during the injection process are significant (e.g., pressure dropping from 10 MPa to 5 MPa), making them easily observable and of practical significance. This also indicates that the method proposed by the author and their team, based on the principle of stress seepage, for the advanced exploration of depleted zones through water injection, is feasible.

4. Conclusions

Through theoretical analysis and on-site water injection experiments, this study investigated the disturbance and stress changes around goaf areas (old galleries) and the feasibility of using water injection to explore these areas. The following conclusions were drawn:

(1) Theoretical analysis suggests that when the equivalent normal stress caused by groundwater in fractured rock masses is greater than zero, the permeability of the fractures will significantly increase. The presence of disturbance and stress reduction zones around goaf areas (old galleries) provides a theoretical basis for using water injection to detect these areas.
(2) On-site water injection experiments showed that regardless of whether the boreholes were directed towards the goaf or the old galleries, the closer they were to these areas, the lower the water injection pressure and the higher the permeability.
(3) Based on the water injection pressure and permeability data from the experiments, and referencing previous theories, the goaf areas (old galleries) were divided into three zones: the original intact zone, the stress relief zone, and the disturbance zone.
(4) The experiments demonstrated that the significant reduction in pressure and increase in permeability during water injection were easily observable, indicating practical significance.

Author Contributions: Conceptualization, J.X.; methodology, H.Z.; software, H.Z.; validation, Y.L. and C.W.; formal analysis, H.Z.; investigation, B.D.; resources, B.D.; data curation, Y.L. and C.W.; writing—original draft preparation, H.Z.; writing—review and editing, J.X.; visualization, B.D.; supervision, H.Z.; project administration, J.X.; funding acquisition, J.X. All authors have read and agreed to the published version of the manuscript.

Funding: This research was funded by the General Program of the National Natural Science Foundation of China (NO. 52274243).

Data Availability Statement: The data used to support the findings of this study are included within the manuscript.

Conflicts of Interest: Author Bing Dong was employed by the company Anhui Wanbei Coal Power Group Co., Ltd. The remaining authors declare that the research was conducted in the absence of any commercial or financial relationships that could be construed as a potential conflict of interest.

References

1. Dong, S. Discussion on several key scientific problems of frequent coal mine floods in China. *Coal J.* **2010**, *35*, 66–71.
2. Zhao, T. *Typical Coal Mine Water Disaster Cases and Prevention Technology*; China University of Mining and Technology Press: Xuzhou, China, 2006; pp. 28–63.
3. Guo, Y. Cause analysis and prevention measures of goaf water disaster. *Chin. J. Saf. Sci.* **2006**, *16*, 140–144.
4. Hou, X.; Yang, T.; Li, Z.; Sun, Y.; Jin, Y. Types and main characteristics of goaf water disaster in Shanxi Province. *J. Min. Saf. Eng.* **2020**, *37*, 1010–1015.
5. Jin, D.; Liu, Y.; Liu, Z. New progress in research on prevention and control technology of major water inrush disasters in coal mines. *Coal Sci. Technol.* **2013**, *41*, 24–27.
6. Zhang, B.; Duan, X.; Yin, S. Research on comprehensive exploration and prevention technology of goaf water. *J. North China Inst. Sci. Technol.* **2016**, *13*, 10–13.
7. Zhou, D.; Zhang, Y.; Chen, Y. Innovation and application of geophysical exploration methods for metal deposits. *World Nonferrous Met.* **2024**, *16*, 133–135.
8. Yang, F. Hydrogeological Structure Model and Disaster Mechanism of Goaf Water Inrush in Shanxi Province. Master's Thesis, University of Mining and Technology, Xuzhou, China, 2019; pp. 1–4.
9. Lekontsev, Y.M.; Sazhin, P.V. Application of the directional hydraulic fracturing at Berezovskaya Mine. *J. Min. Sci.* **2008**, *44*, 253–258. [CrossRef]
10. Wu, Q. *Interpretation of Water Prevention and Control Rules for Coal Mines*; Coal Industry Press: Beijing, China, 2018; pp. 75–77.
11. Analysis of the '10·25' large water disaster accident in Xigu County Coal Industry, Changzhi Xiang Coal Mine. *Shanxi China Coal News*, 16 May 2020; 4th ed.
12. Illman, W.A. Strong field evidence of directional permeability scale effect in fractured rock. *J. Hydrol.* **2006**, *319*, 227–236. [CrossRef]
13. Kortas, L.; Younger, P.L. Fracture patterns in the Permian Magnesian Limestone Aquifer, Co. Durham, UK. *Proc. Yorks. Geol. Soc.* **2013**, *59*, 161–171. [CrossRef]
14. Lomize, G.M. *Flow in Fractured Rocks*; Gesenergoizdat: Moscow, Russia, 1951.
15. Sheng, J.; Su, B. Review of seepage-stress coupling in fractured rock mass. *Geomechanics* **1998**, *19*, 92–95.
16. Wang, W.; Sui, W.; Dong, Q. Effect of stress recovery on permeability evolution of mining-induced fractured rock mass. *Coal J.* **2014**, *39*, 1031–1038.
17. Chen, Y.-F.; Liu, M.M. Non-Darcy's law-based analytical models for data interpretation of high-pressure packer tests in fractured rocks. *Eng. Geol.* **2015**, *199*, 91–106. [CrossRef]
18. Xu, J.; Gui, H. Analysis and experimental study on characteristics of activated water conductivity of mining-induced faults. *J. China Univ. Min. Technol.* **2012**, *41*, 415–418.
19. Qin, Q. Experimental and Numerical Studies on Seepage-Deformation Coupling of Deep-Buried Rock Fractures. Master's Thesis, China University of Geosciences, Wuhan, China, 2011.
20. Zhao, Y.; Yang, D.; Zheng, S.; Hu, Y. Experimental study on physical properties of water seepage in rock fracture under three-dimensional stress. *Sci. China Ser. E-Technol. Sci.* **1999**, *29*, 82–86.
21. Wang, H.; Ren, F.; Liu, D. Experimental study on the influence of triaxial stress on the seepage characteristics of single fractured sandstone. *J. Civ. Eng.* **2023**, *56*, 122–133.
22. Chen, Y.; Lu, S. *Surrounding Rock Control of Coal Mine Roadway in China*; China University of Mining and Technology Press: Xuzhou, China, 1994; pp. 136–137.
23. Zhu, J.; Wu, J.; Shi, J. *Study on Deformation Mechanism and Control Technology of Gob-Side Roadway*; China University of Mining and Technology Press: Xuzhou, China, 2018; pp. 24–25.
24. Yi, S.-H.; Tian, Z.-T.; Wang, H. Research on the identification method of directional lead drilling encountered void area based on the theory of unconfirmed measurement. *J. North China Inst. Sci. Technol.* **2020**, *17*, 67–72.
25. *NB/T 35113-2018*; Specification for Water Pressure Test in Borehole of Hydropower Projects. National Energy Administration: Beijing, China, 2018.